

Dynamic Silos: Modularity in intra-organizational communication networks during the Covid-19 pandemic

Jonathan Larson¹, Tiona Zuzul², Emily Cox Pahnke³, Neha Parikh Shah⁴, Patrick Bourke⁵, Nicholas Caurvina⁶, Fereshteh Amini⁷, Youngser Park⁸, Joshua Vogelstein⁹, Jeffrey Weston¹⁰, Christopher White¹¹, and Carey E. Priebe¹²

¹Microsoft Research

²University of Washington Foster School of Business

³University of Washington Foster School of Business

⁴Microsoft

⁵Microsoft Research

⁶Microsoft Research

⁷Microsoft

⁸Johns Hopkins University

⁹Johns Hopkins University

¹⁰Microsoft

¹¹Microsoft Research

¹²Johns Hopkins University

*cep@jhu.edu

ABSTRACT

Workplace communications around the world were drastically altered by Covid-19, work-from-home orders, and the rise of remote work. We analyze aggregated, anonymized metadata from over 360 billion emails within over 4000 organizations worldwide to examine changes in network community structures from 2019 through 2020. We find that, during 2020, organizations around the world became more siloed, evidenced by increased modularity. This shift was concurrent with decreased stability, indicating that organizational siloes had less stable membership. We provide initial insights into the implications of these network changes – which we term dynamic silos – for organizational performance and innovation.

1 Introduction

How has the Covid-19 pandemic altered intra-organizational communication networks? To answer this question, we analyze data on 362 billion aggregated email receipts between more than 1.4 billion email accounts in 4361 organizations across multiple countries/regions during 2019 and 2020[†]. We examine both the volume of emails between employees in the same organization, and the network structures that can be observed from their exchange¹. We find that, in the spring of 2020, the volume of emails increased globally, but stayed the same or even decreased within some organizations. At the same time, organizations across the globe became more siloed, as evidenced by increased modularity. The promise of remote work is that it expands the boundaries of who can communicate with whom, and should therefore facilitate more connectedness in organizations. Yet changes in monthly modularity — considered in conjunction with shifts in the adjusted Rand index (ARI), a measure of the stability of community structures — suggest that as employees moved to remote work in response to Covid-19, intra-organizational email communication networks became more siloed. We conceptualize these shifts as dynamic silos, and discuss the implications of our findings — the idea that small world communities within companies became more siloed in response to Covid-19 — for organizational performance and innovation around the globe².

Organizational communication networks facilitate essential exchanges of information and support. Covid created exceptional circumstances that disrupted work in many ways never before observed on such a scale. Shifting ways of working — driven by Covid-related changes such as widespread stay at home orders and increased corporate support for remote work — radically altered the ways that employees communicated with each other. By identifying patterns in who communicates with whom, we can identify network structures within an organization and how they changed during the pandemic. One measure of the structure within a network is modularity. Modularity captures the strength of division of a network into communities, or the extent to which a network structure exhibits siloing. Highly modular networks are one form of small worlds². At high levels of modularity, networks display well defined silos that are largely separated from others. At low levels, networks display less-well defined communities, and greater levels of connectivity across the overall network.

Modularity³⁻⁵ is defined as $Q(G) = \max_{\tau} \frac{1}{L} \sum_{u,v \in V} (A_{u,v} - \frac{d_u d_v}{L}) I\{\tau_i = \tau_j\}$ where A denotes the adjacency matrix, d_v denotes the vertex degree, $L = \sum_v d_v$, and $\tau \in [K]^n$ encodes a network partition assigning n vertices to K communities. The Leiden algorithm⁶ is used to find a network partition that approximately maximizes the modularity function.

We also consider ARI⁷. Given a network on the same set of n nodes at two different times, G_t and $G_{t'}$, and letting P_t and $P_{t'}$ be partitions of the two networks into communities, the Rand index is defined as $RI(G_t, G_{t'}) = (a + b) / \binom{n}{2}$ where a is the number of pairs of nodes that are in the same subset in both P_t and $P_{t'}$ and b is the number of pairs of nodes that are in different subsets in both partitions. ARI adjusts this measure for chance, so that $ARI \approx 0$ indicates that which nodes cluster together is essentially chance across the two networks, while $ARI \approx 1$ indicates that individual nodes' community memberships are stable across the two networks. We calculate ARI using the maximum modularity partitions.

While dynamic network structure is a complicated concept, we can begin to understand the interplay between modularity and ARI by considering simplified cases. For example, in stochastic blockmodels⁸ (SBMs) with both the number and the size of the blocks held constant, an increase in Q together with a small value of ARI implies (1) more clearly delineated groups together with (2) significant group membership churn.

Consider two graphs, G_1 and G_2 . Both are SBMs with $K = 2$ blocks, $n = 20$ vertices, and 10 vertices per block; the only difference is in the block connectivity matrices B_1 and B_2 , which are of the form $[b_{11}, b_{12}; b_{21}, b_{22}]$. Furthermore, we assume the within-block connectivities $b_{11} = b_{22} = 0.50$ for both B_1 and B_2 , but the between-block connectivity is $b_{12} = b_{21} = 0.15$ for B_1 decreasing to 0.05 for B_2 . In this case, the network structure measure modularity $Q(G_2)$ is larger than $Q(G_1)$: $Q(G_1) = 0.400 \pm 0.035$ vs. $Q(G_2) = 0.266 \pm 0.035$. If also we assume that the block memberships are altered such that two of the ten members of block one from G_1 switch to block two in G_2 , replaced by two from G_1 's block two moving to G_2 's block one, then the block membership stability measure $ARI(G_1, G_2) = 0.324$. This behavior is illustrated in Figure 1: the modularity increase indicates fracturing of the internal community structure, and the corresponding decrease in stability indicates that the communities themselves experience membership churn.

Organizational scholars have identified consistently high levels of modularity (.60-.75) in the collaboration networks of firms in the television⁹, microelectronics¹⁰, computing^{11,12}, and Biotech/Pharma¹⁰ industries. These findings indicate that inter-organizational networks are characterized by well-defined communities.

To our knowledge, prior research has not measured modularity in intra-organizational communication networks and has not examined how modularity shifts over time. We attribute this gap to data limitations, as a comparative and dynamic analysis of network structure requires longitudinal data within and across many organizations. The breadth and scope of our data provides unprecedented insight into intra-organizational network structures around the world and over time. We find that modularity within companies is relatively stable and high across geographies: modularity ranges from 0.66-0.69 in Canada to

[†]We analyzed workplace trends that were anonymized by aggregating the data broadly. We never observe nor use customer content — such as information within an email — in the data analysis. All personal and organization-identifying information, such as company name, were removed from the data before analysis.

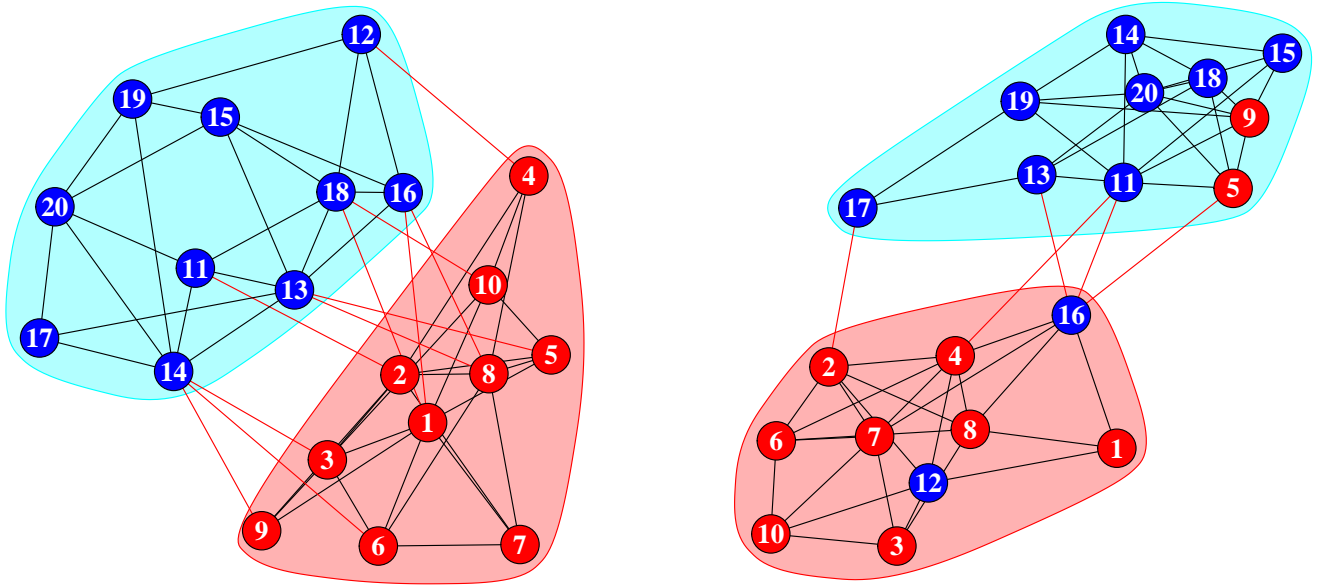


Figure 1. Illustrative network change example. Depicted is a network observed at two time points, G_1 (left) and G_2 (right), representing two time points for a single organization, each with twenty nodes and two communities. The vertex colors denote block membership in G_1 , so we can see that two vertices change communities. The shaded communities are the Leiden-derived maximum modularity communities. The two networks have the same within-community connectivity but G_2 has lower between-community connectivity (fewer red edges) than G_1 ; the network structure measure modularity yields $Q(G_2) = 0.41 > Q(G_1) = 0.30$ indicating fracturing of the internal community structure. Furthermore, community membership of some nodes changes from G_1 to G_2 ; the community membership stability measure $ARI(G_1, G_2) = 0.324$ indicating that the communities themselves experience membership churn. The intra-organizational networks we consider, while vastly more complex, exhibit similar behavior coincident with the onset of Covid-19.

0.75-0.77 in Germany, and 50% of all organizations fall within the 0.64-0.77 range. But, by overlaying monthly modularity from 2019 with 2020, we also observe that modularity increased within organizations in the spring of 2020. To better understand this shift in modularity, we also examine changes in community stability (ARI). Together, our data indicate that – despite baseline differences in network structures – intra-organizational email communication networks across the world became more dynamically siloed following Covid-19.

2 Network time series data

A network or graph G consists of a vertex set V of actors and an edge set E of interactions: $G = (V, E)$. We consider *undirected* and *weighted* networks, so each edge $e \in E$ is a pair $(u, v) \in V \times V$ together with a scalar weight $w_e \in \mathfrak{R}$. The networks considered herein are human communication graphs as observed in an organizational context. We begin with anonymized communications data for approximately 100,000 organizations over a period of 29 months, from Jul 2018 through Nov 2020 – a total of approximately 450 billion email receipts. For this analysis, we use aggregated monthly email communication to define our networks. For each organization i and each month t , we construct an undirected weighted edge (u, v) with the weight $w_{i,t,(u,v)}$ being the total number of messages observed between accounts u and v . (To filter out company-wide messages and broader communications, no email with more than 4 recipients is considered[†]. In addition, we eliminate self-loops: edges from u to u are ignored.) This edge definition induces a undirected weighted graph from which we extract the largest (weakly) connected component, denoted $G_{i,t} = (V_{i,t}, E_{i,t})$ where $V_{i,t}$ is the collection of accounts and edge $(u, v) \in E_{i,t}$ indicates that accounts u and v had at least one message between them. We restrict attention to only those organizations i with $|V_{i,t}| > 2000$ for all t , yielding 4,361 organization network time series and a total of $4361 \cdot 29 = 126,469$ organization-month networks including a total of approximately 362 billion email receipts. By construction, all networks have at least 2000 nodes; the largest networks have approximately 500,000 nodes. We also investigate a separate organization, Microsoft (MSFT), with networks defined the same way for Jan 2019 through Dec 2020. MSFT is one of the larger organizations, with approximately 80,000 nodes in the monthly largest connected components. Analyzing the data was computationally intensive and required the use of large scale distributed compute infrastructure; in all, it took over 55,000 compute hours for clustered machines to process the email data.

For illustration, Figure 2 presents a network map of MSFT for Mar 2020. The figure shows the entire organization ($n = 80,690$) with modularity $Q_{MSFT,MAR2020} = 0.82$ (top), along with top-level sub-organizations with high modularity $Q = 0.85$ (bottom left) and low modularity $Q = 0.79$ (bottom right).

Figure 3 provides a histogram summarizing the modularity $Q(G_{i,t})$ for all 126,469 organization-month networks. Figure 3 also includes two country/region-specific histograms (Canada and Germany), showing clearly that country/region is a confounder in this overall histogram (as are time and network size). Finally, Figure 3 includes modularities for four individual networks in the MSFT organization, showing that Feb 2019, Mar 2019, and Feb 2020 are all approximately the same but Mar 2020 exhibits increased modularity. (Numerical details for these four MSFT months are presented in Section 3 Table 1.)

Figure 4 summarizes network size vs. modularity for all 126,469 organization-month networks, and includes the four MSFT months (investigated in Section 3) as well as Canada and Germany (investigated in Section 4). We also include a selection of publicly available networks, for context.

In the remainder of the paper, we investigate the networks for the MSFT organization in detail in Section 3, and we investigate the collection of 4361 organizations in Section 4. We conclude with a discussion of and initial insights into the implications of the network changes we observe – dynamic silos – for organizational efficiency and innovation.

[†]Our approach mirrors other research in excluding mass emails¹³; we also examined cutting off the number of recipients at 2, 3 and 7 recipients, with largely similar results.

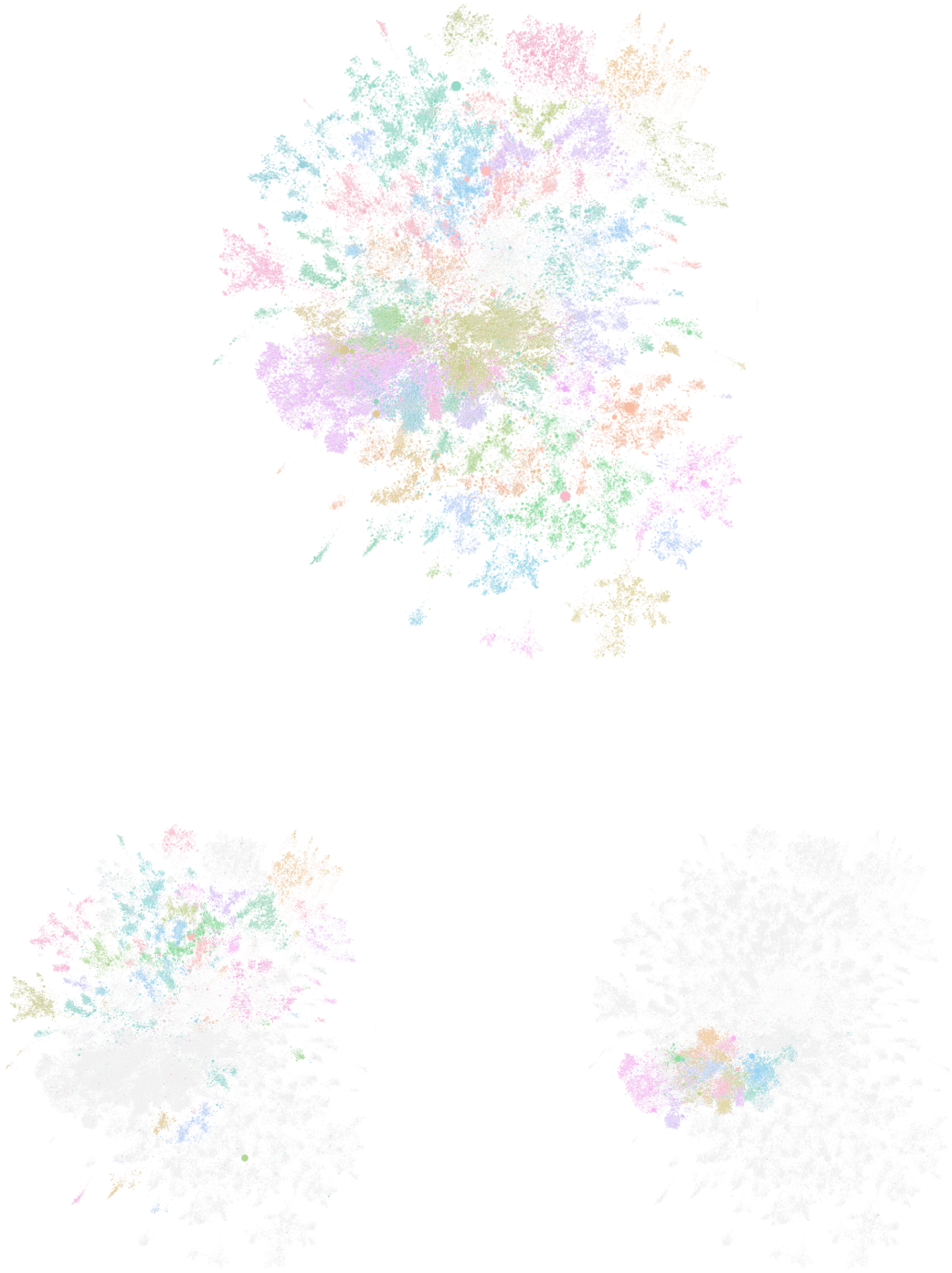


Figure 2. For illustration, we present one representation of $G_{MSFT,Mar2020}$, the MSFT network for Mar 2020. Colors distinguish communities as discovered via the maximum modularity partition. Top: the entire organization, with $n = 80,690$ nodes and modularity $Q = 0.82$. Using formal organizational chart data to isolate entire top-level sub-organizations, we present in the bottom two panels sub-organizations with high modularity (left SubOrg 5, with $n = 29,958$ and $Q = 0.85$) and low modularity (right SubOrg 2, with $n = 10,243$ and $Q = 0.79$).

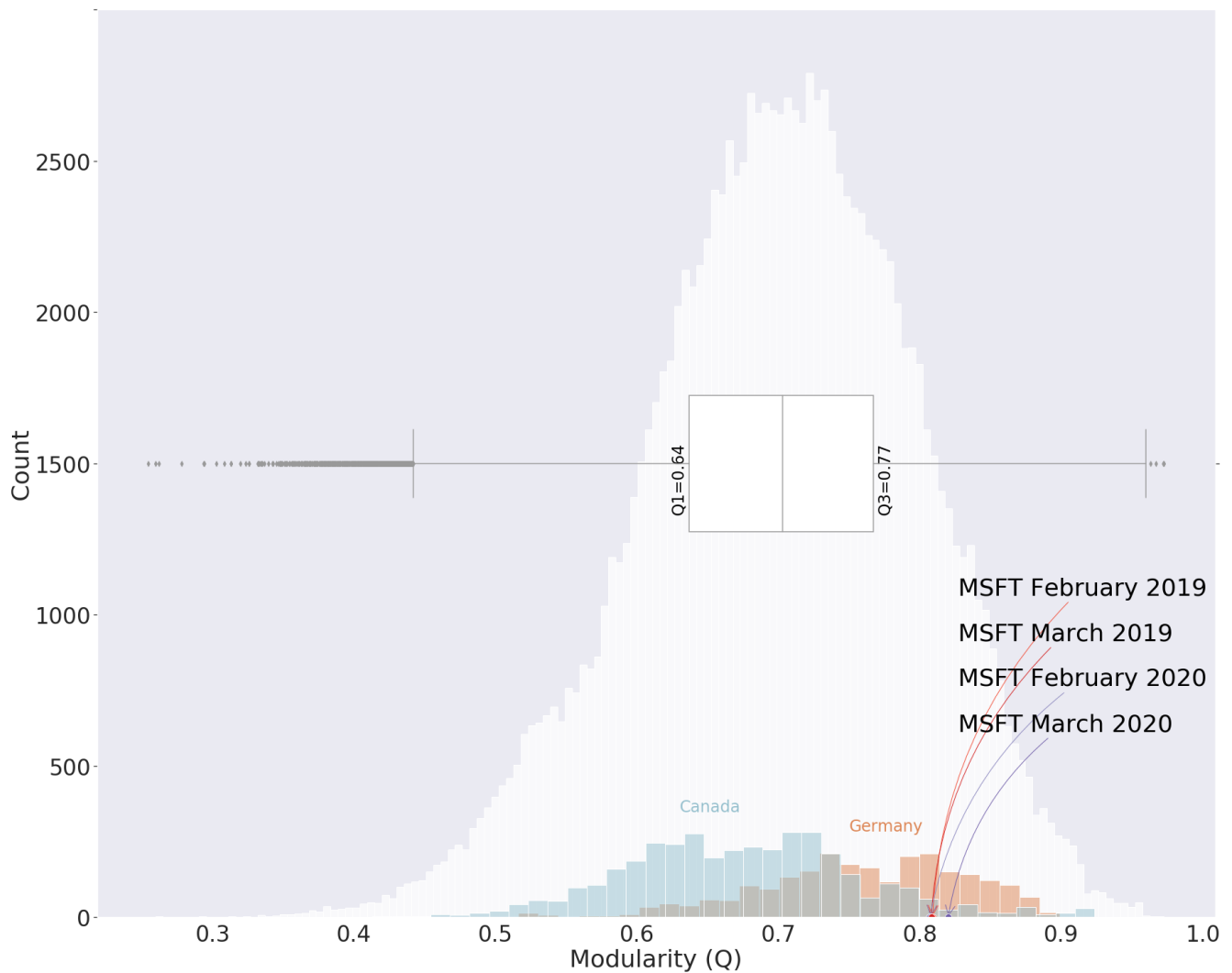


Figure 3. Modularity histogram and boxplot for all 126,469 organization-month networks, with interquartile range (0.64,0.77). The two sub-histograms represent Canada (blue) and Germany (green), indicating a geography effect. The dots on the x-axis represent individual MSFT networks for four months: Feb 2019 & Mar 2019 (red) and Feb 2020 & Mar 2020 (purple), indicating an increase in modularity in spring 2020 coincident with March 4 issuance of work from home order for the company due to Covid-19.

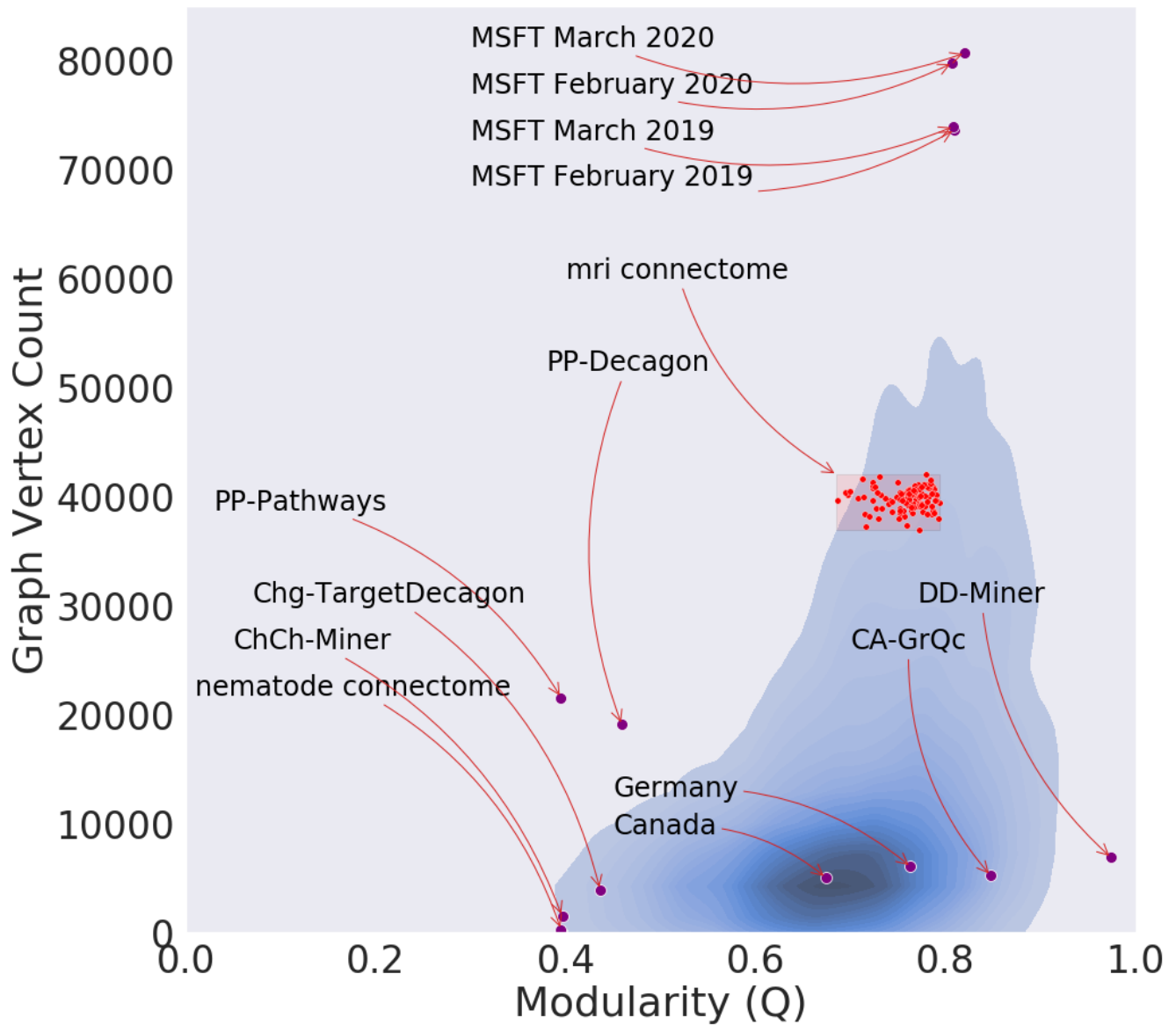


Figure 4. Heatmap for a kernel density estimate of network size n versus modularity Q for the 126,469 organization-month networks depicted via histogram in Figure 3. Individual dots for four MSFT months are included, along with median modularity vs. median network size for Canada and Germany. For context, we compare a selection of other publicly available networks.

3 MSFT

The MSFT organization data yields a time series of networks consisting of 24 months, from Jan 2019 through Dec 2020.

Figure 2 presents a network layout illustration for MSFT Mar 2020 with modularity $Q = 0.82$ (along with a high-modularity suborganization and a low-modularity suborganization).

Figure 3 highlights modularity for MSFT Feb 2019, Mar 2019, Feb 2020, and Mar 2020. We see an increased modularity in Mar 2020. Figure 4 includes modularity Q vs. network size n for these four MSFT months $G_{MSFT,t}$. Table 1 presents numerical details for these four MSFT months. In particular, $\Delta Q(G_{MSFT, Feb2019}, G_{MSFT, Mar2019}) = Q(G_{MSFT, Mar2019}) - Q(G_{MSFT, Feb2019}) = -0.001$ while $\Delta Q(G_{MSFT, Feb2020}, G_{MSFT, Mar2020}) = 0.013$; the spring 2020 change is an order of magnitude large than the spring 2019 change.

	number of nodes	number of edges	total weight of all edges	modularity
Feb 2019	73,625	1,688,952	14,520,982	0.809
Mar 2019	73,946	1,603,704	12,401,940	0.808
Feb 2020	79,764	1,805,376	13,923,141	0.807
Mar 2020	80,690	1,879,892	16,460,603	0.820

Table 1. Basic network statistics, including modularity, for MSFT Feb 2019, Mar 2019, Feb 2020, and Mar 2020.

Figure 5 presents the histogram of non-zero weights for March 2020 – note that this figure is on a log scale for both axes – as well as monthly average weighted degree. This figure indicates that, besides an initial spike in the spring of 2020, the volume of emails did not increase within MSFT.

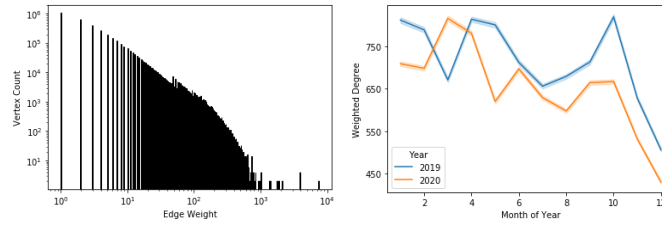


Figure 5. Left: Histogram of nonzero weights for MSFT March 2020. Right: Average weighted degree for all vertices vs. time.

Figure 6 plots modularity (left panel) and ARI (right panel) as a function of time for the full MSFT time series of networks. Both the modularity increase and ARI decrease in spring 2020 coinciding with Covid-19 are clear: Q increases from Feb to Mar to Apr to May and ARI plummets for Apr vs. May. NB: ARI for May vs. Jun going back up means that the new group membership structure stayed in place: groups membership structure changes from Apr to May, but remains stable from May to Jun. (This same phenomenon is present in data for the 4361 organizations – see Figure 9 Section 4.)

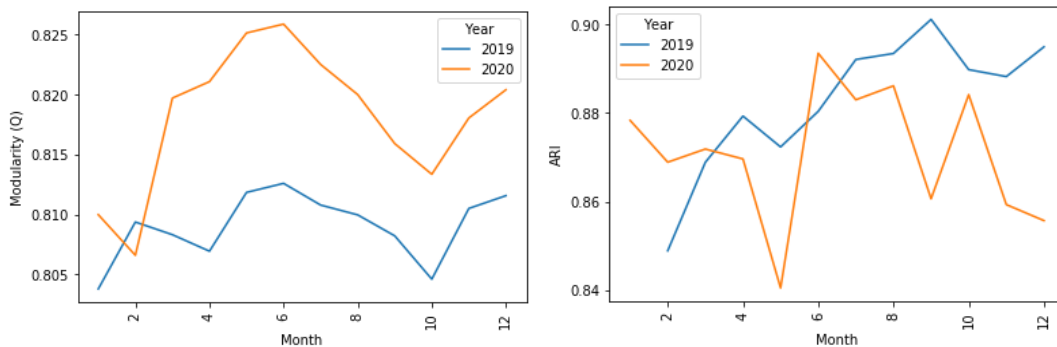


Figure 6. Modularity $Q(G_{MSFT,t})$ (left) and month-over-month adjusted Rand index $ARI(G_{MSFT,t}, G_{MSFT,t-1})$ (right) as a function of time for the MSFT networks from Jan 2019 through Dec 2020. A spring 2020 increase in modularity coupled with a decrease in ARI is evident.

To assess the significance of the MSFT modularity change we observe from Feb 2020 to Mar 2020 (see Table 1 and Figure 6 left panel) we consider network bootstrapping¹⁴. For Feb 2020 the observed modularity is $Q = 0.807$ and the bootstrap yields $Q = 0.804 \pm 0.0037$; for Mar 2020 the observed modularity is $Q = 0.820$ and the bootstrap yields $Q = 0.818 \pm 0.0035$.

3.1 MSFT top-level sub-organizations

Figures 7 and 8 investigate top-level sub-organizations within the overall MSFT organization as defined via the formal organizational chart for Feb 2019 vs Mar 2019 and Feb 2020 vs Mar 2020 in terms of the change in modularity $\Delta Q = Q(G_{MSFT,t}) - Q(G_{MSFT,t'})$ and the $ARI(G_{MSFT,t} - G_{MSFT,t'})$. The histogram presented in Figure 7 shows the number of nodes for Mar 2020. (Sub-organizations 2 and 5 were considered in the network map presented in Figure 2.) The scatter plot presented in Figure 8 shows (1) the modularity changes for 2019 are small (± 0.005 for all seven sub-organizations) while for 2020 the modularity changes are much larger (and all positive except for sub-organization 3), and (2) the ARIs are mostly in the same range for the two years except for sub-organization 3.

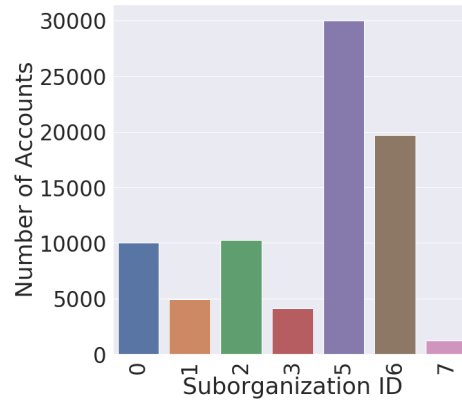


Figure 7. Histogram for number of nodes for seven MSFT top-level sub-organizations.

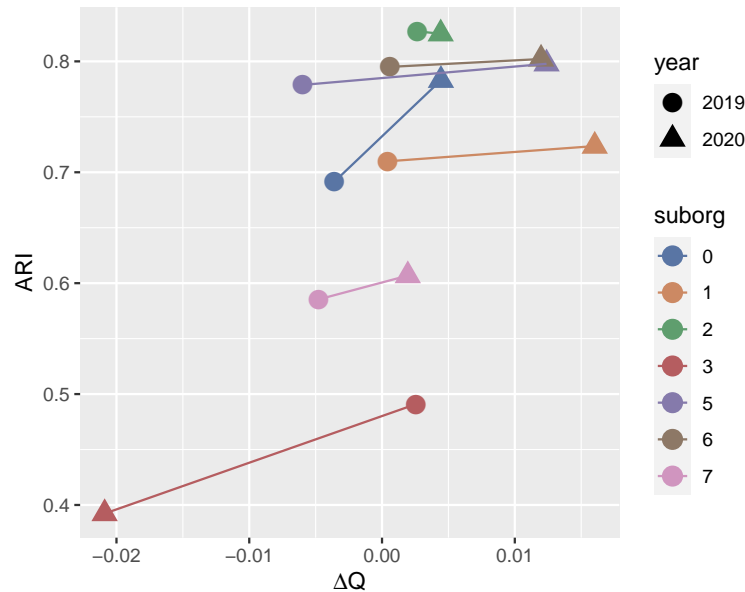


Figure 8. Scatter plot for seven MSFT sub-organizations indicating changing behavior between Feb 2019 vs Mar 2019 and Feb 2020 vs Mar 2020. We see, for instance, that six of the seven experienced an increased modularity change in 2020 vs 2019. Suborg 3, which dropped in modularity significantly, includes members of Microsoft’s strategy and operations organization, manning the organization’s control center through the crisis. Members of this critical group very nimbly adapted their networks to current needs. They did so by paring down connections within their own working group and keeping and forming connections across groups, likely to those only most acutely relevant to regain stability for the organization and its employees.

4 4361 Organizations

We now investigate the time series of networks for 4361 organizations. We now investigate the time series of networks for 4361 organizations. As described in more detail in Section 2, these organizations are located worldwide and have from 2000 to 500000 email accounts each. We observe email receipts across the networks for 29 months, resulting in 126,469 organization-month networks. The breadth of the data in terms of organization size, location, and type, together with the duration of time, provides sufficient coverage to enable insights into global trends related to changes in intra-organizational email communication patterns throughout 2019 and 2020.

Figure 9 shows monthly modularity $\{Q(G_{i,t})\}_{i \in 1, \dots, 4361}$ and month-over-month community stability $\{ARI(G_{i,t}, G_{i,t-1})\}_{i \in 1, \dots, 4361}$ for the 4361 organization networks at each time t . Figure 10 depicts volume vs. time for this data set. Unlike within MSFT, the volume of emails increased in 2020. As was apparent for MSFT – see Figure 6 Section 3 – the increase in modularity and decrease in ARI in spring 2020 is clear.

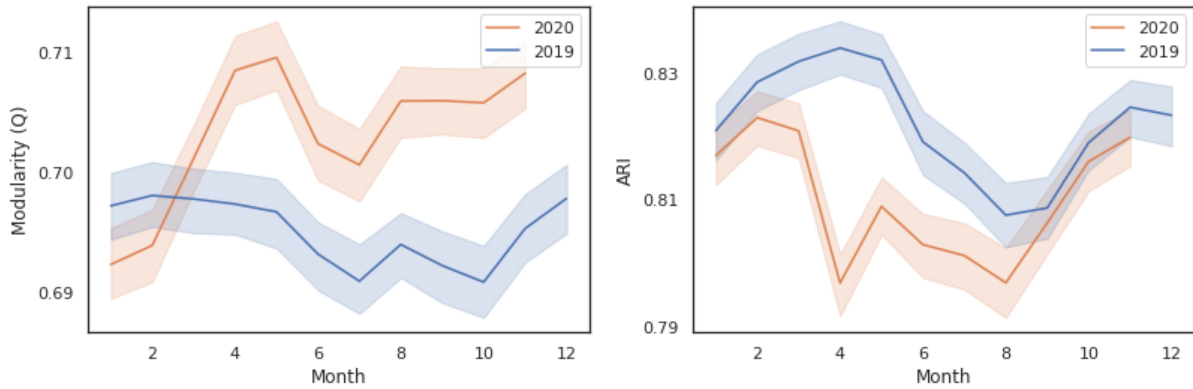


Figure 9. Considering the collection of all 4361 organizations for Jan 2019 - Nov 2020: the left panel shows monthly modularity $Q(G_{i,t})$ (mean \pm one standard error); the right panel shows month-over-month adjusted Rand index $ARI(G_{i,t}, G_{i,t-1})$ (mean \pm one standard error). A change coinciding with Covid-19 is clear: in spring 2020 the modularity increases significantly and there is a corresponding decrease in month-over-month ARI.

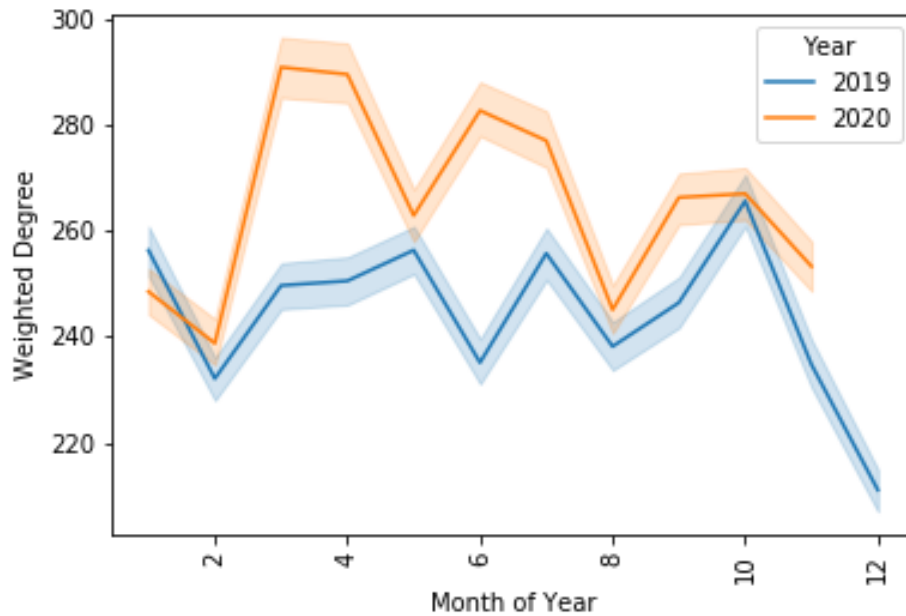


Figure 10. Email volume vs. time for the collection of all 4361 organizations.

Figure 11 presents a quantitative analysis of the spring 2020 modularity increase apparent in Figure 9 (left panel): the paired Wilcoxon test shows that year-over-year modularity is clearly increased for post-Covid-19 Apr 2020 compared to Apr 2019 (two-sided Wilcoxon p -value ≈ 0), as opposed to no significant difference for pre-Covid-19 Jan 2020 compared to Jan 2019. We obtain a similar result (p -value ≈ 0) for the Covid-19-associated ARI change apparent in Figure 9 (right panel).

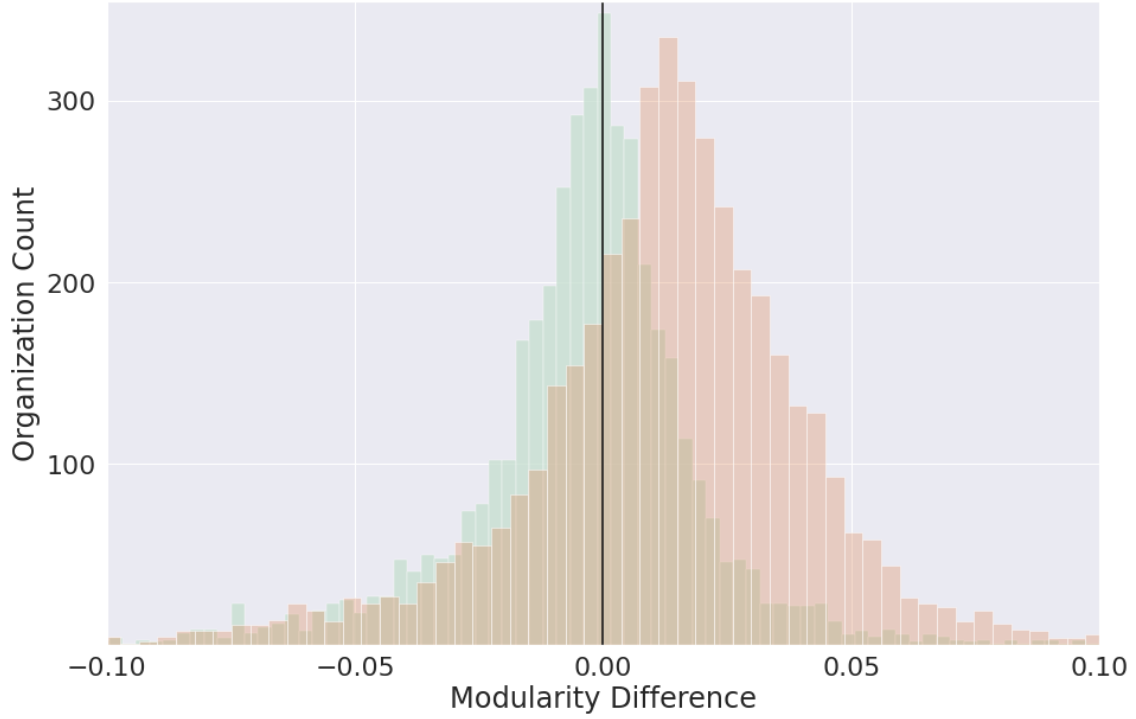


Figure 11. Year-over-year modularity paired difference histograms $Q(G_{i,t}) - Q(G_{i,t'})$ for all 4361 organization networks i at times t and $t' = t$ minus one year. Green: Jan 2020 - Jan 2019, centered near zero (no statistically significant difference in modularity Jan 2020 compared to Jan 2019). Red: Apr 2020 - Apr 2019, centered greater than zero (increased modularity Apr 2020 compared to Apr 2019; two-sided Wilcoxon p -value ≈ 0) indicating a Covid-19 effect.

Further examining the modularity for all organizations presented in aggregate in Figure 3 and by time in Figure 9, Figure 12 presents modularity aggregated by geography for Canada and Germany – time series versions of these histograms presented in Figure 3. While the modularity for Germany is consistently larger than that for Canada, in both cases we see a modularity increase in spring 2020. The number of organizations considered in Figure 12 is $N_{Canada} = 132$ and $N_{Germany} = 84$. Histograms of network sizes for both countries/regions are shown in Figure 13, corresponding to medians of n vs. Q depicted in Figure 4. Figure 14 presents modularity as a function of time for ten additional countries/regions, showing similar trends. Table 2 shows modularity values for 12 countries/regions for April 2019 and April 2020.

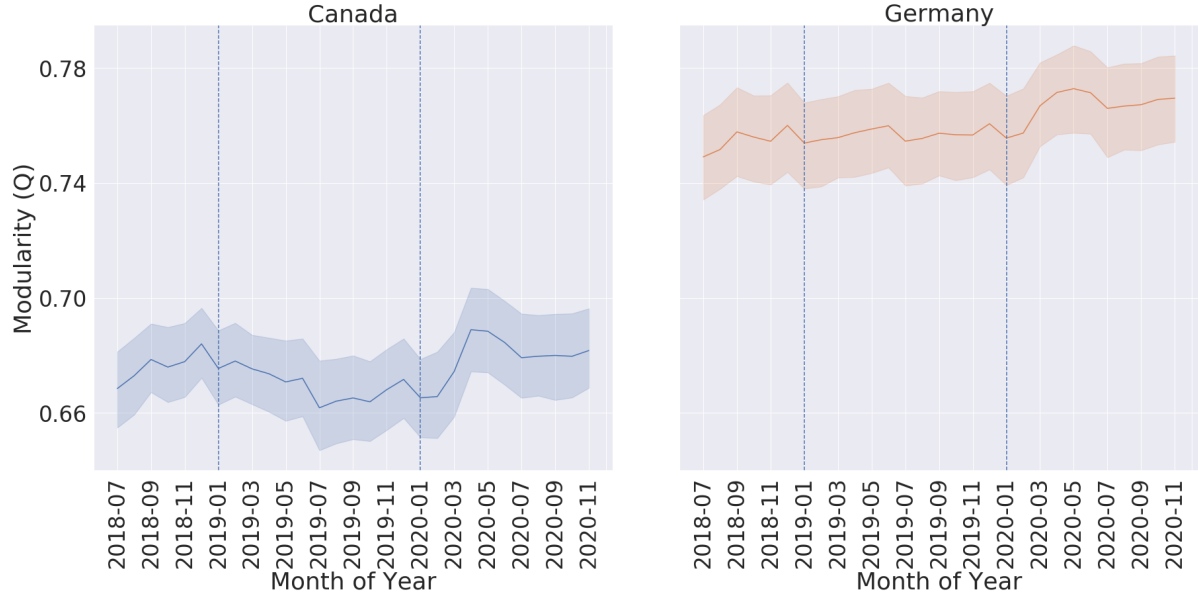


Figure 12. Monthly modularity vs. time $Q(G_{i,t})$ (mean \pm one standard error) for organizations i in Canada (left) and Germany (right).

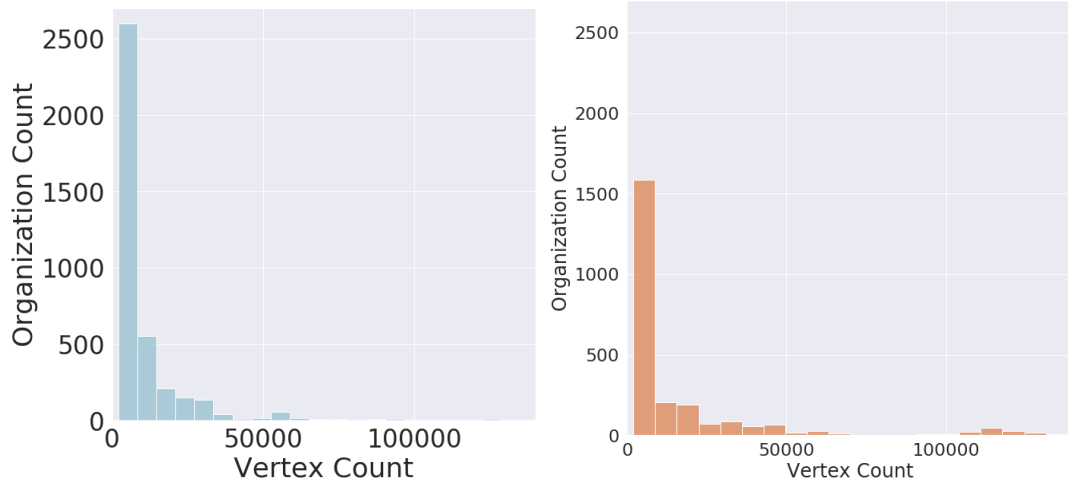


Figure 13. Histograms of network sizes for Canada (132 organizations) and Germany (84 organizations). The median number of nodes for Canada is 5046 and for Germany is 6039.

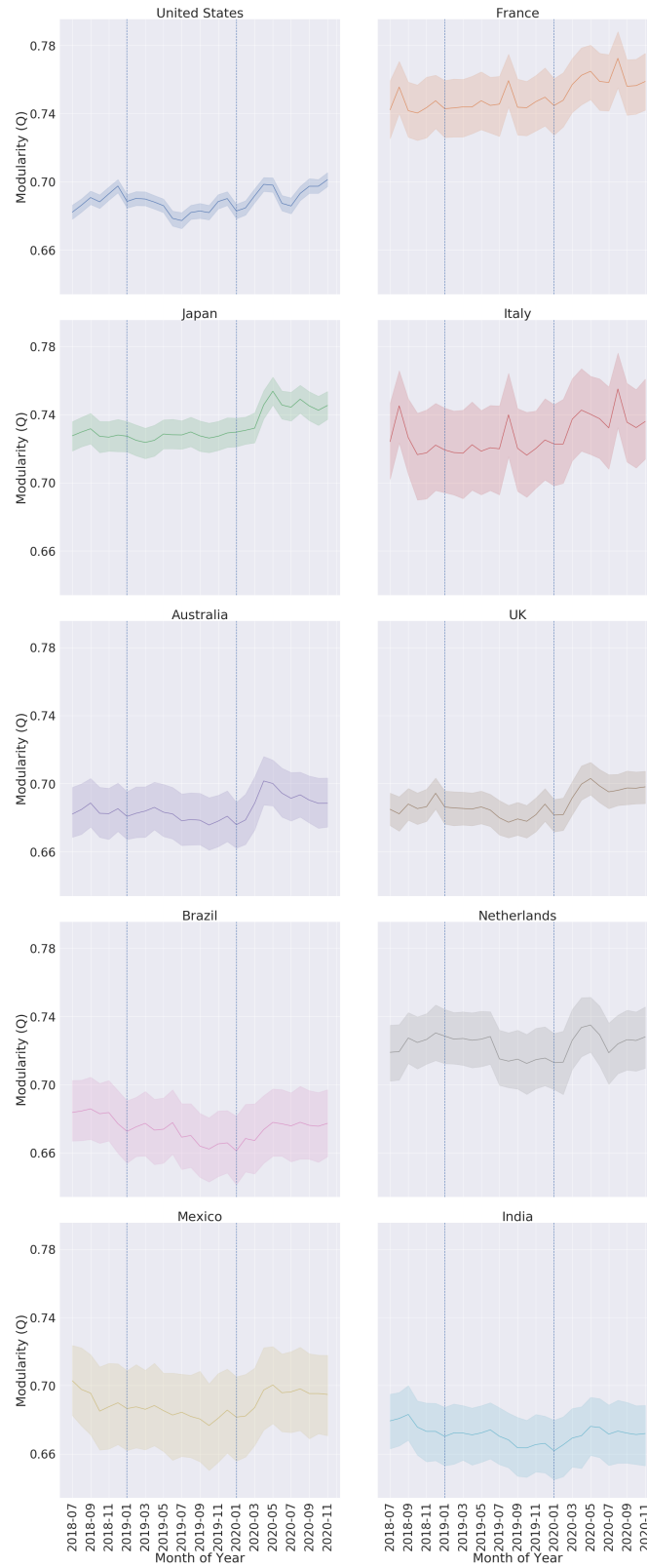


Figure 14. Monthly modularity vs. time $Q(G_{i,t})$ (mean \pm one standard error) for ten additional countries/regions.

	Mean Modularity April 2019	Mean Modularity April 2020	ΔQ
Canada	0.674	0.689	0.015
Germany	0.757	0.771	0.014
Australia	0.686	0.702	0.016
Brazil	0.673	0.673	0.000
France	0.744	0.763	0.019
India	0.671	0.671	0.000
Italy	0.722	0.742	0.020
Japan	0.725	0.746	0.021
Mexico	0.688	0.697	0.009
Netherlands	0.726	0.734	0.008
UK	0.685	0.700	0.015
United States	0.688	0.698	0.010

Table 2. Mean modularity change by country/region, Apr 2019 vs. Apr 2020.

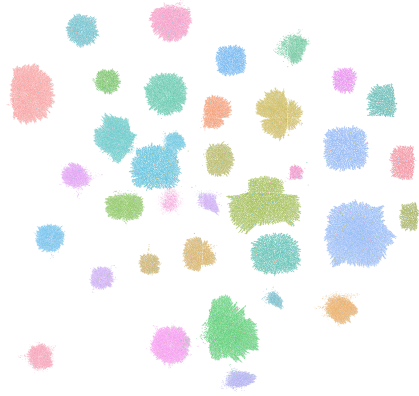
Returning to Figure 3, we see now, in light of the investigations presented in Sections 3 and 4, that the overall histogram of modularity confounds modularity differences associated with number of nodes and time and geography. Nonetheless, whether looking at the full collection of 4361 organizations, or aggregated by country/region, or the MSFT network in particular, we see consistently a spring 2020 increase in modularity and decrease in ARI. Specifically: for MSFT the maximum modularity over time is achieved in Jun 2020 and the minimum ARI is achieved for Apr vs. May, while for the 4361 organizations the maximum modularity is achieved in May 2020 and the minimum ARI is achieved for Mar vs. Apr; the behavior is generally analogous, but with MSFT delayed one month.

5 A Generative Model

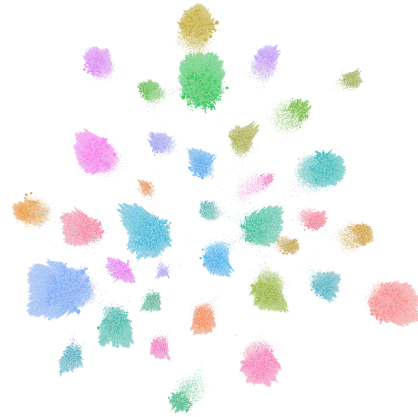
Access, privacy, and legal considerations often prohibit obtaining raw communication data for analysis. In an effort to facilitate future research and analysis of human communications within organizational structures, we have created a generative model designed for our intra-organizational communication networks. We propose a generalization of the Barabasi-Albert¹⁵ generative model for the networks considered herein: a Barabasi-Albert augmented hierarchical stochastic block model (BA-HSBM). Figure 15 presents a visual comparison of this new model with its simpler competitors. This provides fitted generative models for all 126,469 organization-month networks, enabling independent research to be conducted into organizational behavior and providing baselines for comparisons against observed activity.

We start with root level Leiden community structures and create an a posteriori stochastic block model that retains the population statistics for both vertices and edges from the real network being fit. In addition, to make Barabasi-Albert fit well in the context of an SBM, we modify the algorithm: within each block of the SBM, we consider a specific budget of vertices and edges, obtained from the observed network being fit. We configure the Barabasi-Albert algorithm to create a number of edges for each vertex equal to the intra-block average degree centrality. Then, employing either Erdos-Renyi (Figure 15 panel (a)) or Barabasi-Albert (Figure 15 panel (b)) for creation of intra-block connections, we observe major differences between the resulting networks and the real network being fit (Figure 15 panel (d)). The inter-block connections are made at a rate determined by the real network, but the connections are made between random vertices across pairs of communities. We observe the power-law distribution of the degree centrality is much closer to the real network's distribution when using the Barabasi-Albert generator, and the network paths generated using Barabasi-Albert are longer than those generated using Erdos-Renyi. These longer paths produce less regularity in the structures and also allow for some bleed-over between communities as highly eccentric nodes connected to multiple communities will be pulled between those communities.

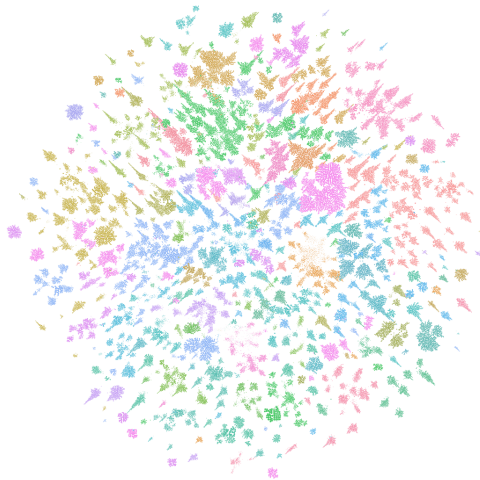
Using these observations, we extend our model to use hierarchical Leiden communities obtained by running Leiden recursively on the real network until we attain leaf communities no larger than n_{max} vertices. (We use $n_{max} = 250$.) Using these leaf communities, we apply the Barabasi-Albert algorithm again for the leaf intra-block connections and then proceed with inter-block connections between leaf clusters. This has the effect of localizing connections between communities to small groups of nodes, which dramatically fractures the network structure (Figure 15 panel (c)), corresponding to the structure observed in the real network being fit: as in the real network, we observe that the generative model now produces many new and small communities. Applying Leiden to data generated from this new generative model, we find that these groups of communities are captured in the same partition when maximizing modularity at the root level, indicating that the more complex and realistic structure generated by BA-HSBM has similar modularity characteristics to the real network being fit, as desired.



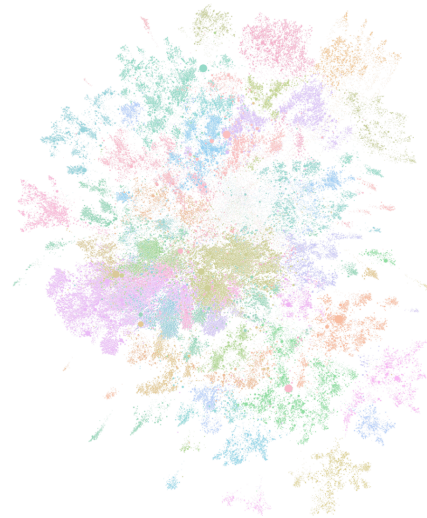
(a) Root-Leiden SBM



(b) Root-Leiden Barabasi-Albert SBM



(c) BA-HSBM



(d) Observed $G_{MSFT,Mar2020}$

Figure 15. Illustrative representations of generative models for $G_{MSFT,Mar2020}$, the MSFT network for Mar 2020.

6 Discussion

In 2020 relative to 2019, intra-organizational email communication networks across countries/regions exhibited increased modularity. At the same time, ARI decreased across organizations. Our analysis shows that organizational networks around the world became more siloed and that the communities within these networks became less stable. Collectively, the widespread shifts in these measures — that is, dynamic silos — have important implications for organizations around the world.

First, these changes might be associated with productivity and efficiency gains. Collaborating with people that have similar domain knowledge¹⁶ or shared interpretive schemas¹⁷ fosters trust¹⁸, facilitates cooperation^{19,20}, and allows for rapid sharing of information and tacit knowledge²¹, fueling efficiency²² and creating enduring interpersonal ties²³. Research has suggested that these benefits can be present even in the face of membership instability or churn, provided that members are assigned clear roles within their groups²⁴. Thus, depending on work practices and features of collaborative groups, dynamic siloing may improve efficiency²⁵.

Second, dynamic siloing may result in lower rates of innovation within some organizations. Innovation often results through novel combinations of distantly held knowledge^{26–29}. Interdisciplinary or cross-department collaborations provide access to new ties and information that can provide fertile material for innovative ideas^{30,31}. If employees limit communication to smaller, more insular groups comprised of members who are similar to one another, they might decrease their ability to access and recombine diverse information and knowledge that might aid in innovation^{12,32,33}.

Finally, increased modularity in large organizations might be associated with a specific kind of innovation: the development of competence-destroying technologies^{34,35}. Competence-destroying technologies create new product classes and render existing organizational capabilities obsolete, and are typically initiated by new firms^{36,37} or small teams³⁸. Within large or incumbent organizations, competence-destroying, architectural, or disruptive innovation is best developed by teams or workgroups with few connections to the rest of the organization^{39–41}. Increased modularity might foster the cultural separation and autonomy necessary for teams to develop this kind of innovation. Thus, dynamic siloing might be associated with positive – and counterintuitive – shifts in innovation within large, established organizations.

We hope this research will stimulate future studies connecting modularity and related measures in communication networks to organizational outcomes. Our analysis highlights the need for future studies examining the drivers and implications of geographic differences both in baseline modularity scores, and in the magnitude of post-Covid-19 modularity shifts. If these shifts are associated with changes in organizational performance and innovation, they may have implications for national competitiveness and resilience, and merit continued focus as organizational communities evolve after the pandemic. We also found that modularity increased both within MSFT (where email volume remained similar in 2020 to 2019) and worldwide (where email volume increased). We see potential for studies to explore the link between volume of communication and network structure. Finally, recent studies have shown that, as a result of Covid-related work-from-home orders, employees transferred their informal interactions to new forms of digital communication, including instant messages⁴². While we focus on email data, future studies can examine the network structures revealed by multi-modal changes in communications via video conferencing, social media or chat data.

As leaders begin to better understand the modularity of their own organizations, they might be strategic about how to capture the benefits while mitigating potential downsides of dynamic silos. Overall, we suggest that when the worlds within organizations become more siloed, they need not become less fertile.

Data Availability

An anonymized version of the data presented on Microsoft Corporation supporting this study will be retained indefinitely for scientific and academic purposes. The data are available from the authors upon reasonable request and with permission of Microsoft Corporation.

Code Availability

The code used to produce the results shown on Microsoft, and the code used to create the generative models as well as fitted generative models for all 126,469 organization-month networks, are available upon reasonable request and with permission of Microsoft Corporation.

References

1. Jacobs, A. Z. & Watts, D. J. A large-scale comparative study of informal social networks in firms. *Manag. Sci.* **0**, DOI: [10.1287/mnsc.2021.3997](https://doi.org/10.1287/mnsc.2021.3997) (2021).
2. Watts, D. J. & Strogatz, S. H. Collective dynamics of ‘small-world’ networks. *Nature* **393**, 440–442, DOI: [10.1038/30918](https://doi.org/10.1038/30918) (1998).
3. Newman, M. E. J. & Girvan, M. Finding and evaluating community structure in networks. *Phys. Rev. E* **69**, 026113, DOI: [10.1103/PhysRevE.69.026113](https://doi.org/10.1103/PhysRevE.69.026113) (2004).
4. Newman, M. E. J. Modularity and community structure in networks. *Proc. Natl. Acad. Sci.* **103**, 8577–8582, DOI: [10.1073/pnas.0601602103](https://doi.org/10.1073/pnas.0601602103) (2006).
5. Bickel, P. J. & Chen, A. A nonparametric view of network models and newman–girvan and other modularities. *Proc. Natl. Acad. Sci.* **106**, 21068–21073, DOI: [10.1073/pnas.0907096106](https://doi.org/10.1073/pnas.0907096106) (2009).
6. Traag, V., Waltman, L. & van Eck, N. J. From Louvain to Leiden: guaranteeing well-connected communities. *Sci. Reports* **9**, DOI: [10.1038/s41598-019-41695-z](https://doi.org/10.1038/s41598-019-41695-z) (2019).
7. Hubert, L. & Arabie, P. Comparing partitions. *J. Classif.* **2**, 193–218 (1985).
8. Holland, P. W., Laskey, K. B. & Leinhardt, S. Stochastic blockmodels: First steps. *Soc. Networks* **5**, 109–137, DOI: [https://doi.org/10.1016/0378-8733\(83\)90021-7](https://doi.org/10.1016/0378-8733(83)90021-7) (1983).
9. Clement, J., Shipilov, A. & Galunic, C. Brokerage as a Public Good: The Externalities of Network Hubs for Different Formal Roles in Creative Organizations. *Adm. Sci. Q.* **63**, 251–286, DOI: [10.1177/0001839217708984](https://doi.org/10.1177/0001839217708984) (2018).
10. Tatarynowicz, A., Sytch, M. & Gulati, R. Environmental Demands and the Emergence of Social Structure: Technological Dynamism and Interorganizational Network Forms. *Adm. Sci. Q.* **61**, 52–86, DOI: [10.1177/0001839215609083](https://doi.org/10.1177/0001839215609083) (2016).
11. Sytch, M. & Tatarynowicz, A. Exploring the Locus of Invention: The Dynamics of Network Communities and Firms’ Invention Productivity. *Acad. Manag. J.* **57**, 249–279, DOI: [10.5465/amj.2011.0655](https://doi.org/10.5465/amj.2011.0655) (2014).
12. Gulati, R., Sytch, M. & Tatarynowicz, A. The Rise and Fall of Small Worlds: Exploring the Dynamics of Social Structure. *Organ. Sci.* **23**, 449–471, DOI: [10.1287/orsc.1100.0592](https://doi.org/10.1287/orsc.1100.0592) (2012).
13. Kleinbaum, A. M. Organizational misfits and the origins of brokerage in intrafirm networks. *Adm. Sci. Q.* **57**, 407–452, DOI: [10.1177/0001839212461141](https://doi.org/10.1177/0001839212461141) (2012).
14. Green, A. & Shalizi, C. R. Bootstrapping exchangeable random graphs (2017). [arXiv:1711.00813](https://arxiv.org/abs/1711.00813).
15. Barabási, A.-L. & Albert, R. Emergence of scaling in random networks. *Science* **286**, 509–512, DOI: [10.1126/science.286.5439.509](https://doi.org/10.1126/science.286.5439.509) (1999).
16. Simon, H. A. Machine as mind. In *Machines and Thought*, vol. 1, 81–102 (Oxford University Press New York, 1996).
17. Gulati, R. Does Familiarity Breed Trust? The Implications of Repeated Ties for Contractual Choice in Alliances. *Acad. Manag. J.* **38**, 85–112, DOI: [10.5465/256729](https://doi.org/10.5465/256729) (1995).
18. Coleman, J. S. Social Capital in the Creation of Human Capital. *Am. J. Sociol.* **94**, S95–S120, DOI: [10.1086/228943](https://doi.org/10.1086/228943) (1988).
19. Reagans, R. & Zuckerman, E. W. Networks, Diversity, and Productivity: The Social Capital of Corporate R&D Teams. *Organ. Sci.* **12**, 502–517, DOI: [10.1287/orsc.12.4.502.10637](https://doi.org/10.1287/orsc.12.4.502.10637) (2001).
20. Wang, D., Pahnke, E. C. & McDonald, R. The Past Is Prologue? Venture-Capital Syndicates, Collaborative Experience and Start-Up Exits. *Acad. Manag. J.* **amj.2019.1312**, DOI: [10.5465/amj.2019.1312](https://doi.org/10.5465/amj.2019.1312) (2021).

21. Granovetter, M. Economic Action and Social Structure: The Problem of Embeddedness. *Am. J. Sociol.* **91**, 481–510, DOI: [10.1086/228311](https://doi.org/10.1086/228311) (1985).
22. Reagans, R. & McEvily, B. Network Structure and Knowledge Transfer: The Effects of Cohesion and Range. *Adm. Sci. Q.* **48**, 240–267, DOI: [10.2307/3556658](https://doi.org/10.2307/3556658) (2003).
23. Dahlander, L. & McFarland, D. A. Ties That Last: Tie Formation and Persistence in Research Collaborations over Time. *Adm. Sci. Q.* **58**, 69–110, DOI: [10.1177/0001839212474272](https://doi.org/10.1177/0001839212474272) (2013).
24. Valentine, M. A. & Edmondson, A. C. Team Scaffolds: How Mesolevel Structures Enable Role-Based Coordination in Temporary Groups. *Organ. Sci.* **26**, 405–422, DOI: [10.1287/orsc.2014.0947](https://doi.org/10.1287/orsc.2014.0947) (2015).
25. Choudhury, P. R., Foroughi, C. & Larson, B. Work, “from, anywhere”: The productivity effects of geographic flexibility. *Strateg. Manag. J.* **42**, 655–683, DOI: [10.1002/smj.3251](https://doi.org/10.1002/smj.3251) (2021).
26. Schumpeter, J. A. & Opie, R. *The theory of economic development: an inquiry into profits, capital, credit, interest, and the business cycle*. No. vol. XLVI in Harvard economic studies (Harvard University Press, Cambridge, Mass, 1934).
27. Kogut, B. & Zander, U. Knowledge of the Firm, Combinative Capabilities, and the Replication of Technology. *Organ. Sci.* **3**, 383–397, DOI: [10.1287/orsc.3.3.383](https://doi.org/10.1287/orsc.3.3.383) (1992).
28. Hargadon, A. & Sutton, R. I. Technology Brokering and Innovation in a Product Development Firm. *Adm. Sci. Q.* **42**, 716–749, DOI: [10.2307/2393655](https://doi.org/10.2307/2393655) (1997).
29. Burt, R. Structural Holes and Good Ideas. *Am. J. Sociol.* **110**, 349–399, DOI: [10.1086/421787](https://doi.org/10.1086/421787) (2004).
30. Soda, G. B., Mannucci, P. V. & Burt, R. Networks, Creativity, and Time: Staying Creative through Brokerage and Network Rejuvenation. *Acad. Manag. J.* *amj.2019.1209*, DOI: [10.5465/amj.2019.1209](https://doi.org/10.5465/amj.2019.1209) (2021).
31. Rawlings, C. M., McFarland, D. A., Dahlander, L. & Wang, D. Streams of Thought: Knowledge Flows and Intellectual Cohesion in a Multidisciplinary Era. *Soc. Forces* **93**, 1687–1722, DOI: [10.1093/sf/sov004](https://doi.org/10.1093/sf/sov004) (2015).
32. Uzzi, B. Social Structure and Competition in Interfirm Networks: The Paradox of Embeddedness. *Adm. Sci. Q.* **42**, 35–67, DOI: [10.2307/2393808](https://doi.org/10.2307/2393808) (1997).
33. Tortoriello, M., Reagans, R. & McEvily, B. Bridging the Knowledge Gap: The Influence of Strong Ties, Network Cohesion, and Network Range on the Transfer of Knowledge Between Organizational Units. *Organ. Sci.* **23**, 1024–1039, DOI: [10.1287/orsc.1110.0688](https://doi.org/10.1287/orsc.1110.0688) (2012).
34. Abernathy, W. J. & Clark, K. B. Innovation: Mapping the winds of creative destruction. *Res. Policy* **14**, 3–22, DOI: [10.1016/0048-7333\(85\)90021-6](https://doi.org/10.1016/0048-7333(85)90021-6) (1985).
35. Tushman, M. L. & Anderson, P. Technological Discontinuities and Organizational Environments. *Adm. Sci. Q.* **31**, 439–465, DOI: [10.2307/2392832](https://doi.org/10.2307/2392832) (1986).
36. Tripsas, M. Unraveling the process of creative destruction: Complementary assets and incumbent survival in the typesetter industry. *Strateg. Manag. J.* **18**, 119–142 (1997).
37. Zuzul, T. & Tripsas, M. Start-up Inertia versus Flexibility: The Role of Founder Identity in a Nascent Industry. *Adm. Sci. Q.* **65**, 395–433, DOI: [10.1177/0001839219843486](https://doi.org/10.1177/0001839219843486) (2020).
38. Wu, L., Wang, D. & Evans, J. A. Large teams develop and small teams disrupt science and technology. *Nature* **566**, 378–382, DOI: [10.1038/s41586-019-0941-9](https://doi.org/10.1038/s41586-019-0941-9) (2019).
39. Henderson, R. M. & Clark, K. B. Architectural Innovation: The Reconfiguration of Existing Product Technologies and the Failure of Established Firms. *Adm. Sci. Q.* **35**, 9–30, DOI: [10.2307/2393549](https://doi.org/10.2307/2393549) (1990).
40. Christensen, C. M. *The innovator’s dilemma: when new technologies cause great firms to fail*. The management of innovation and change series (Harvard Business School Press, Boston, Mass, 1997).
41. Benner, M. J. & Tushman, M. L. Exploitation, Exploration, and Process Management: The Productivity Dilemma Revisited. *The Acad. Manag. Rev.* **28**, 238, DOI: [10.2307/30040711](https://doi.org/10.2307/30040711) (2003).
42. Yang, L. *et al.* How Work From Home Affects Collaboration: A Large-Scale Study of Information Workers in a Natural Experiment During COVID-19. *arXiv:2007.15584 [cs]* (2020).